# Observation of Nonlinear Effects in Compton Scattering

C. Bula, K. T. McDonald, and E. J. Prebys
*Joseph Henry Laboratories, Princeton University, Princeton, New Jersey 08544*

C. Bamber,* S. Boege, T. Kotseroglou, A. C. Melissinos, D. D. Meyerhofer,† and W. Ragg
*Department of Physics and Astronomy, University of Rochester, Rochester, New York 14627*

D. L. Burke, R. C. Field, G. Horton-Smith, A. C. Odian, J. E. Spencer, and D. Walz
*Stanford Linear Accelerator Center, Stanford University, Stanford, California 94309*

S. C. Berridge, W. M. Bugg, K. Shmakov, and A. W. Weidemann
*Department of Physics and Astronomy, University of Tennessee, Knoxville, Tennesee 37996*
(Received 4 December 1995)

Nonlinear Compton scattering has been observed in the collision of a low-emittance 46.6-GeV electron beam with terawatt pulses from a Nd:glass laser at 1054 and 527 nm wavelengths in an experiment at the Final Focus Test Beam at SLAC. Peak laser intensities of $10^{18}$ W/cm$^2$ have been achieved, corresponding to a value of 0.6 for the parameter $\eta = e\mathcal{E}_{\rm rms}/m\omega_0 c$. Results are presented for multiphoton Compton scattering in which up to four laser photons interact with an electron, in agreement with theoretical calculations. [S0031-9007(96)00012-9]

PACS numbers: 41.60.–m, 12.20.Fv, 42.65.Vh

Considerations of the interaction of electrons with intense wave fields [1–7] led to the introduction of the dimensionless measure of field strength

$$\eta = \frac{e\mathcal{E}_{\rm rms}}{m\omega_0 c} = \frac{e\mathcal{E}_{\rm rms}\lambda_0/2\pi}{mc^2} = \frac{e\sqrt{\langle A_\mu A^\mu\rangle}}{mc^2}, \quad (1)$$

for a plane wave of laboratory frequency $\omega_0$, wavelength $\lambda_0$, root-mean-square electric field $\mathcal{E}_{\rm rms}$, and four-vector potential $A_\mu$. Here $e$ and $m$ are the charge and mass of the electron, respectively, and $c$ is the speed of light. A field with $\eta = 1$ has a voltage drop of $2\pi mc^2/e \approx 3$ MV per laser wavelength. The classical radiation spectrum for $\eta \ll 1$ includes the $n$th harmonic of the wave frequency $\omega_0$ (multipole radiation) at relative strength $\eta^{2n}$, which is nonlinear in wave intensity for $n > 1$. In the quantum view this corresponds to absorption of several wave photons accompanied by emission of a single photon of frequency $\omega$:

$$e + n\omega_0 \longrightarrow e' + \omega\,. \quad (2)$$

Only one observation of this effect has been reported: a weak signal of second-harmonic radiation in scattering of 1-keV electrons from a $Q$-switched Nd:YAG laser [8].

We report on an experiment in which 46.6-GeV electrons are scattered at the focus of an intense laser with wavelength $\lambda_0 = 1054$ (infrared) and 527 nm (green). In the rest frame of the electron beam, the corresponding incident photon energies are 211 and 421 keV, respectively, so the recoil of scattered electrons is significant, and the interaction (2) can be described as Compton scattering. At the laser intensities achieved ($I \approx 10^{18}$ W/cm$^2$, $\eta \approx 0.6$) nonlinear effects were readily observed.

In this experiment the scattered electrons were detected. When an electron of initial energy $E_0$ absorbs $n$ photons from a laser pulse with intensity parameter $\eta$ and crossing angle $\theta_0$ to the electron beam, the minimum energy of the scattered electron is $E_{\rm min} = E_0/[1 + ns/\overline{m}^2c^4]$ where $s = 2E_0\omega_0(1 + \cos\theta_0)$. This expression utilizes the effective mass, $\overline{m} = m\sqrt{1 + \eta^2}$, of electrons in a strong wave field that arises due to "dressing" by continual absorption and re-emission of wave photons [6,9]. For ordinary (linear) Compton scattering ($n = 1, \eta \ll 1$) the minimum scattered-electron energy is 25.6 GeV at $E_0 =$ 46.6 GeV and $\theta_0 = 17°$. The spectrum of scattered electrons corresponding to $n > 1$ extends below 25.6 GeV, permitting an identification of multiphoton Compton scattering.

Electrons with energy below 25.6 GeV also occur when the electron independently scatters twice or more as it traverse the laser focus. We refer to this process as multiple Compton scattering, and it is physically distinct from nonlinear Compton scattering in which several photons are absorbed at a single point, but only a single high-energy photon is emitted. The interaction length in the laser focus is approximately $\lambda_0/\alpha\eta^2$, where $\alpha$ is the fine-structure constant. Electrons that passed through the focal region had a 1/4 probability of interacting, and 1/16 scattered twice, etc.

Figure 1 shows spectra of scattered electrons calculated according to Ref. [5] for conditions representative of the present experiment with $\eta = 0.5$. This semiclassical calculation is based on the Volkov solutions [7,10] to the Dirac equation, and differs from one based on a quantized laser field only in radiative corrections [6]. The calculation includes the space-time profiles of the electron and laser beams and makes the adiabatic approximation that the rate based on infinite plane waves holds for the

 0031-9007/96/76(17)/3116(4)$10.00 

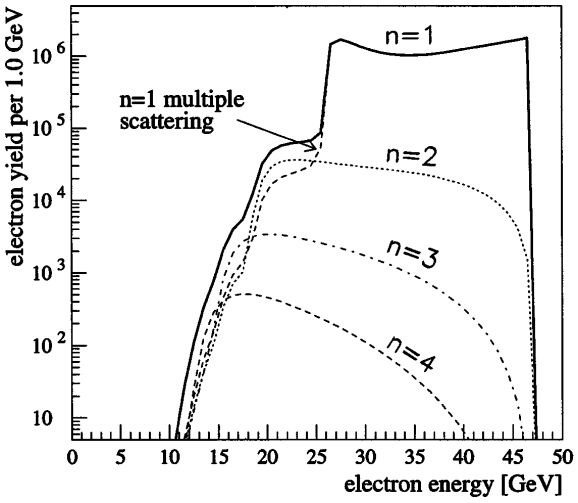


FIG. 1. Calculated yield of scattered electrons from the collision of $5 \times 10^9$ 46.6-GeV electrons with a circularly polarized 1054-nm laser pulse of intensity parameter $\eta = 0.5$.

local value of $\eta$. The curves in Fig. 1 are labeled by the highest number of photons that are absorbed in a single scattering event. Thus the dashed curve labeled $n = 1$ corresponds to linear Compton scattering, but extends below 25.6 GeV because of multiple Compton scattering. The curve labeled $n = 2$ also extends below the nominal minimum energy for nonlinear Compton scattering because additional linear Compton scatters also occur. The upper solid curve is the sum of all scatterings.

The experiment was carried out in the Final Focus Test Beam at SLAC [11], and is shown schematically in Fig. 2. The laser beam was focused onto the electron beam by an off-axis parabolic mirror of 30-cm focal length with a 17° crossing angle at the interaction point, IP1, 10 m downstream of the Final Focus. A set of permanent magnets was used to direct the electron beam downward to the dump and also served to analyze the momentum of the scattered electrons. Electrons scattered with energy $E \lesssim 30$ GeV were detected in a silicon-tungsten calorimeter (ECAL) that was segmented transversely in 12 rows and 4 columns of $1.6 \times 1.6$ cm$^2$ pads and in four longitudinal groups with 23 radiation lengths total thickness. The calorimeter energy resolution was $\sigma_E/E \approx 0.25/\sqrt{E(\mathrm{GeV})}$, whereas the size of the pads resulted in momentum bins of $\Delta P/P \approx 0.15$. The high-energy

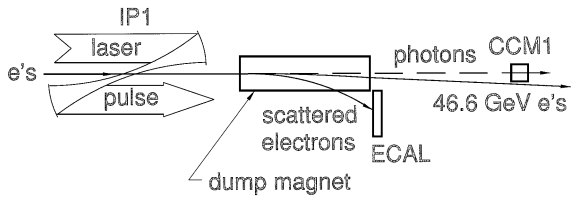


FIG. 2. Schematic drawing of the experiment.

backscattered photons were detected by a gas Čerenkov monitor (CCM1) after conversion in 0.2 radiation length of aluminum. The number of backscattered photons $N_\gamma$ was measured pulse by pulse with a systematic uncertainty of $\pm 10\%$.

The laser was a 1.5-ps, chirped-pulse-amplified Nd:glass terawatt system [12,13] with a relatively high repetition rate of 0.5 Hz achieved by a final laser amplifier with slab geometry [14]. The laser-oscillator mode locker was synchronized to the 476-MHz drive of the SLAC linac klystrons with an observed jitter between the laser and linac pulses of 2 ps (rms) [15].

The peak laser intensity was determined from measurements of the laser energy, focal-spot area, and pulse width. For the infrared laser data all three quantities were measured for every pulse. The uncertainty in the pulse width was $\pm 20\%$ because of diffraction of the laser beam. Fluctuations on the energy probe calibration led to a $\pm 13\%$ uncertainty in the energy measurement. The focal spot area at IP1 was measured by reimaging the focus of the laser on a charge coupled device. Because of laser light scattering, filtering, and a non-Gaussian shape of the focal spot, the uncertainty in the area was $\pm 20\%$. The overall uncertainty in peak intensity was therefore $\pm 30\%$. For the green laser data (obtained by frequency doubling in a KDP crystal), the energy and focal area were measured for each pulse, but the pulse width is known only on average for each data set from streak-camera measurements and varied between $\Delta t = 1.5$ and 2.5 ps. Thus we assign an uncertainty $\Delta I/I = {}^{+0.5}_{-0.3}$ for the green laser data.

The peak focused laser intensity was obtained for infrared pulses of energy $U = 800$ mJ, focal area $A \equiv 2\pi\sigma_x\sigma_y = 60\ \mu\mathrm{m}^2$, and pulse width $\Delta t = 1.5$ ps, for which $I = U/A\Delta t \approx 10^{18}$ W/cm$^2$ at $\lambda_0 = 1054$ nm, corresponding to a value of $\eta = 0.6$.

The electron beam was operated at 10–30 Hz with an energy of 46.6 GeV and emittances $\epsilon_x = 3 \times 10^{-10}$ mrad and $\epsilon_y = 3 \times 10^{-11}$ mrad. The beam was tuned to a focus with $\sigma_x = 60\ \mu$m and $\sigma_y = 70\ \mu$m at the laser-electron interaction point. The electron bunch length was expanded to 3.6 ps (rms) to minimize the effect of the time jitter between the laser and electron pulses. Typical bunches contained $5 \times 10^9$ electrons. However, since the electron beam was significantly larger than the laser focal area, only a small fraction of the electrons crossed through the peak field region.

The spatial and temporal overlap of the electron and laser beams was optimized by observing the Compton scattering rate in the ECAL and CCM1 detectors during horizontal ($x$), vertical ($y$), and time ($t$) scans of one beam across the other. Figure 3 shows results of a combined $x$-$t$ scan. Figure 3(a) is derived from scattered photons and is dominated by linear Compton scattering. The slope of the data agrees with the 17° beam-crossing angle. Figure 3(b) is derived from electrons of energy less than 25.6 GeV where single, linear Compton scattering does

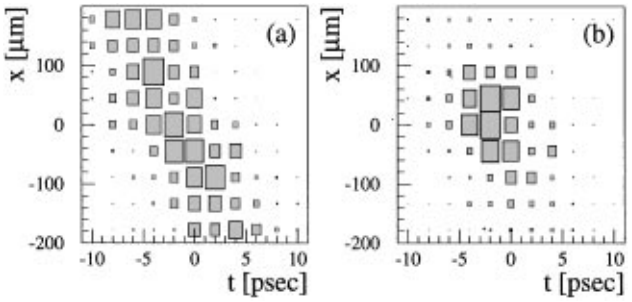


FIG. 3. Observed rates of (a) linear and (b) nonlinear and multiple Compton scattering as a function of $x$ and $t$ offsets between the electron and laser beams. The area of each box is proportional to the signal size.

not contribute. The peak in Fig. 3(b) has a smaller space-time extent than that in Fig. 3(a) because of the stronger dependence of the nonlinear process on laser intensity.

The ECAL sampled the scattered electrons in energy intervals about 2.5 GeV wide. Because of the rapidly decreasing yield at lower energies and the $\approx 100:1$ dynamic range of the ECAL, only data from the top four rows of the calorimeter could be used in the analysis. The highest sampled energy could be adjusted by lowering the entire calorimeter. Thus the complete mapping of the nonlinear Compton spectrum required data collection at several laser intensities and positions of the ECAL.

Data were collected with circularly polarized laser pulses of energies between 14 and 800 mJ at $\lambda_0 = 1054$ nm, and between 7 and 320 mJ at $\lambda_0 = 527$ nm. The energy measured in the calorimeter pads, each of which accepted a limited momentum bite, gave the spectrum of electrons scattered in that pulse. Corrections were applied for shower cross talk between calorimeter pads, and for backgrounds from high-energy Compton-scattered electrons that hit beam-line components. Two methods were used to estimate the corrections, based on shower-spread information from calibration runs and on signals in calorimeter channels outside the acceptance for Compton scattering. The average of the two methods is used, and the difference is taken as a contribution to the systematic uncertainty.

An invariant cross section cannot be defined for nonlinear Compton scattering as it would depend on the laser intensity which varies in space and time. Instead, we discuss the normalized energy spectrum, $(1/N)dN/dE$, of scattered electrons. The total number $N$ of scattered electrons is equal to the total number $N_\gamma$ of high-energy photons (except for corrections of less than 3% due to multiple Compton scattering). The normalized spectrum was deduced for each laser pulse and then averaged to yield the data points in Figs. 4(a) and 5. This technique renders the results less sensitive to the time jitter between the electron and laser pulses and to the consequent uncertainty in the interaction flux.

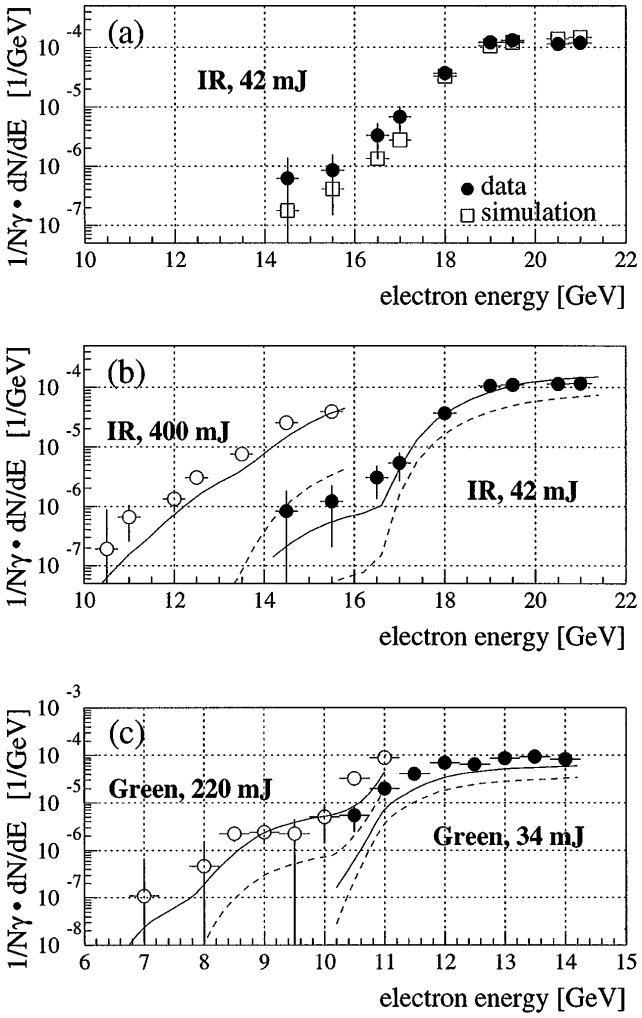


FIG. 4. Energy spectra of scattered electrons as observed in the ECAL calorimeter. (a) Data and simulation for 42-mJ infrared laser pulses. (b), (c) Data (open and filled-in circles) and simulations (solid curves) for infrared (b) and green (c) laser pulses, scaled to standard values of the interaction geometry. The dashed lines show the simulation for multiple linear Compton scattering only.

The spectrum of scattered electrons normalized to the number of Compton $\gamma$ rays is plotted in Fig. 4(a) against the electron energy for data at a nominal laser energy of 42 mJ. The open squares represent a simulation of each pulse using the corresponding laser and electron beam parameters. The simulation includes both nonlinear and multiple Compton scatterings, and combinations of the two. Only energies below the minimum for ordinary Compton scattering are shown. The plateau at 19–21 GeV corresponds to two-photon scatters, and the falloff at 17–18 GeV is evidence for the two-photon kinematic limit at 17.6 GeV as smeared by the momentum resolution of the calorimeter.

To compensate for small variations in the beam parameters during the run, the data in Figs. 4(b) and 4(c) have

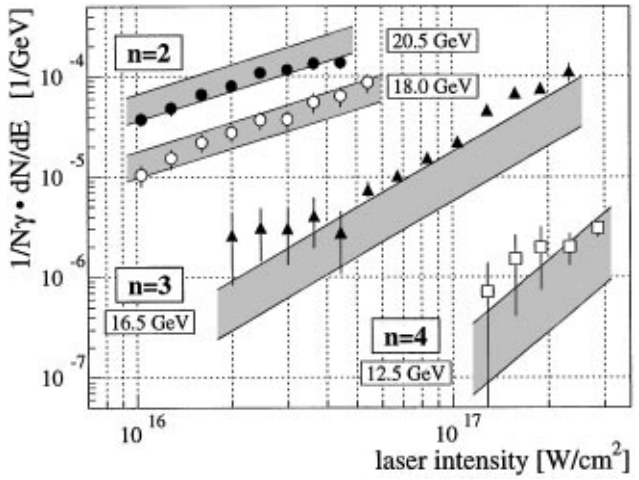


FIG. 5. The normalized yield of scattered electrons of energies corresponding to $n = 2$, 3, and 4 infrared laser photons per interaction versus the intensity of the laser field at the interaction point. The bands represent a simulation of the experiment, including 30% uncertainty in laser intensity and 10% uncertainty in $N_\gamma$.

been scaled by the ratio of the simulated rates at measured and at standard values of electron and laser beam-spot dimensions. For these standard conditions (2 ps laser pulse length, 70 $\mu$m$^2$ laser focal area in the infrared and 35 $\mu$m$^2$ in the green, and electron bunch dimensions $\sigma_x = \sigma_y = 60$ $\mu$m and $\sigma_z = 870$ $\mu$m), the value of $N_\gamma$ is $1.92 \times 10^4$/mJ for the infrared and $0.75 \times 10^4$/mJ for the green laser pulses. Figure 4(b) shows results from infrared data at two laser energies differing by an order of magnitude. The full simulation is shown as the solid curve. The spectrum calculated for multiple linear (i.e., $n = 1$ only) Compton scattering is shown as the dashed curve, which clearly cannot account for the observations. The kinematic limit for $n = 3$ scattering at 13.5 GeV cannot be resolved in the data, but the expected effect is only a very small shoulder in the spectrum.

Figure 4(c) shows similar results from green laser light. The larger experimental uncertainties in this case reflect lower statistics and a larger background subtraction. The $n = 2$ kinematic limit at 10.9 GeV can be discerned in the data. Evidence for the $n = 3$ plateau can be seen in the 220-mJ data.

The error bars shown in Fig. 4(a) represent statistical uncertainty in the number of scattered electrons and systematic uncertainty in the correction for backgrounds in the calorimeter. In Figs. 4(b) and 4(c) and also in Fig. 5 below the error bars also include uncertainties in the scaling to standard beam conditions.

In Fig. 5 we illustrate the rise in the normalized nonlinear yield with infrared-laser intensity. As the yields are normalized to the total Compton-scattering photon signal which is primarily linear Compton scattering, data at electron energies dominated by order $n$ should vary with laser pulse intensity as $I^{n-1}$. The slopes of the four data sets in Fig. 5 agree reasonably well with this expectation, and their magnitudes agree with the simulated yields within the 30% uncertainty in the laser intensity and the 10% uncertainty in $N_\gamma$, shown as a band for each electron energy. The signals for the $n = 2$ and 3 channels are strong, and for laser intensities above $2 \times 10^{17}$ W/cm$^2$ there is good evidence for the $n = 4$ channel.

In conclusion, we have observed nonlinear Compton scattering with the absorption of up to four laser photons in a single scattering event. The spectra of scattered electrons agree within experimental uncertainty with theory [5] at two different laser wavelengths and over a wide range of laser pulse energies.

We acknowledge the support of the SLAC staff. The laser system could not have been completed without support from members of the Laboratory for Laser Energetics at U. Rochester. T. Blalock was instrumental in the construction of the laser system and its installation at SLAC. We also thank U. Haug and T. Koffas for participation in recent data collection, and P. Chen and J. A. Wheeler for many useful conversations. This work was supported in part by DOE Grants DE-FG02-91ER40671, DE-FG02-91ER40685, DE-FG05-91ER40627, and Contract DE-AC03-76SF00515.

*Present address: Hughes Leitz Optical Technologies Ltd., Midland, Ontario, Canada L4R 2H2.
†Department of Mechanical Engineering.

[1] N. D. Sengupta, Bull. Math. Soc. (Calcutta) **44**, 175 (1952).
[2] L. S. Brown and T. W. B. Kibble, Phys. Rev. **133**, A705 (1964).
[3] A. I. Nikishov and V. I. Ritus, Sov. Phys. JETP **19**, 529 (1964); **19**, 1191 (1964); **20**, 757 (1965).
[4] I. I. Gol'dman, Sov. Phys. JETP **19**, 954 (1964); Phys. Lett. **8**, 103 (1964).
[5] N. B. Narozhny *et al.,* Sov. Phys. JETP **20**, 622 (1965).
[6] For a review, see J. H. Eberly, Progress in Optics **VII**, 360 (1969).
[7] V. B. Berestetskii *et al., Quantum Electrodynamics,* 2nd ed. (Pergamon Press, New York, 1982), Secs. 40 and 101.
[8] T. J. Englert and E. A. Rinehart, Phys. Rev. A **28**, 1539 (1983).
[9] T. W. B. Kibble, Phys. Rev. **150**, 1060 (1966).
[10] D. M. Volkov, Z. Phys. **94**, 250 (1935).
[11] V. Balakin *et al.*, Phys. Rev. Lett. **74**, 2479 (1995).
[12] D. Strickland and G. Mourou, Opt. Commun. **55**, 447 (1985).
[13] C. Bamber *et al.,* U. Rochester Report No. UR-1428 (1995).
[14] W. S. Martin and J. P. Chernoch, U.S. Patent 3633126 (1972).
[15] T. Kotseroglou *et al.,* Technical Digest, CLEO '95, CWF51, p. 218.